useful. The stochastic model described previously can be used to develop a better understanding of rockfall motion. Because of the low cost of computer time, it is possible to perform several simulation runs with different random numbers to generate a distribution of the predicted rockfall motion at a given slope segment. Depending on the number of replicates, certain levels of confidence can be achieved. These results can be used as references to determine catchment area width and rock wall location. This model could also be used to evaluate the type of material that should be placed in the catchment area to optimize the investment.

Simulation is a powerful tool for evaluating existing or proposed facilities because it can be used to generate data at low costs. However, extreme caution should be exercised when using any model. The results generated for this project should be verified as appropriate in other areas before they are relied on. As I-40 construction continues, more data will be collected to refine the ROCKSIM model.

ACKNOWLEDGMENTS

The author is indebted to many who have contributed to, and encouraged the development of, this paper. The advice and assistance of John Ledbetter and Naariman Abar of the Soils and Foundation Section of the NCDOT have been major factors in making this paper possible. L.G. Grimes' editorial assistance is also deeply appreciated.

REFERENCES

1. A.M. Ritchie. Evaluation of Rockfall and Its Control. In Highway Research Record 17, HRB, National Research Council, Washington, D.C., 1963, pp. 13-28.
2. D'Appolonia Consulting Engineers, Inc. Rockfall Analyses. North Carolina Department of Transportation and Highway Safety, Raleigh, 1979.
3. D.R. Morton. Slope Stability Problems and Recommendations for Remedial Treatment Along I-40 in the Pigeon River Gorge. North Carolina Department of Transportation and Highway Safety, Raleigh, 1981.

Publication of this paper sponsored by Committee on Engineering Geology.

Stability Charts for Geotextile-Reinforced Walls

DOV LESHCHINSKY and JOHN C. VOLK

ABSTRACT

The results of a mathematical approach to estimate the shear failure resistance of a geotextile-retained soil wall are presented in this paper. The analytical method used is based on a limiting-equilibrium approach combined with variational extremization, and it satisfies all equilibrium requirements. The analytically derived failure mechanism consists of a log-spiral slip surface and reinforcing geotextile sheets positioned orthogonally to the radii defining it. A closed-form solution is obtained that provides complete insight into the problem's behavior. The results indicate that (a) as the geotextile tensile strength increases, the extent of the critical slip surface increases, (b) as the geotextile strength increases, the compressive stress over the critical slip surface also increases, (c) as the geotextile strength increases, the magnitude and extent of tensile normal stress that tends to develop near the top decreases, and (d) when frictional soil is concerned, the strength of the geotextile at the bottom is mobilized the most. The end products are design charts that can easily be applied to a particular problem. The charts indicate that reinforcement may significantly increase the stability of a wall (or slope) depending on the geotextile's tensile strength, the soil's strength properties, and the inclination of the structure face.

In recent years, geotextiles and allied products have been utilized in the construction of retained soil walls. The geotextile sheets are used to wrap compacted soil in layers, thereby producing a stable composite structure. It has been shown that such a construction technique has the potential for a cost-effective substitute for conventional retaining structures (1,2). Geotextile-retained soil walls, referred to in this paper as geotextile-reinforced walls, resemble the popular sandbag walls that have been in use for decades. Contrary to sandbag walls, however, geotextile-reinforced walls can be constructed to significant dimensions because of the geotextile's high strength, its durability, and a simple mechanized construction procedure. A major consideration in the design of a geotextile-reinforced wall is its overall resistance to shear failure that develops through its composite structure. The objective of this paper is to present a simple and consistent analytical tool that is capable of addressing this complex aspect of the problem.

A comprehensive analytical approach to this problem is the finite-element method (3). The soil-geotextile interaction, however, is highly nonlinear and, therefore, a complicated constitutive relationship must be employed in this analysis (4). As a consequence, the application of the finite-element method to standard problems might be too involved and impractical at the present time.

There are currently numerous simplified analysis methods that have been developed to assess the stability of geotextile-reinforced earth structures. Some are an extension of conventional retaining wall theories (5,6) and others are derived from simplified slope stability analysis methods (7-10). Each approach basically utilizes a postulated failure mechanism, that is, an assumed failure surface and the inclination of the geotextile relative to it.

The analytical approach used in this work is founded on the limit equilibrium method combined with extremization utilizing variational calculus. It is free of unnecessary assumptions, satisfies all equations of equilibrium, and is easy to apply. This method is fundamentally an extension of Baker and Garber's approach (11,12). The mathematical details of this extension are shown by Leshchinsky (13) and therefore only a brief description of the analysis is presented here. It should be pointed out, however, that the variational limiting equilibrium approach is equivalent to the upper bound approach of limit analysis where a rigid body failure mechanism is considered (14). The results of this work indicate that although the solution may be considered as an upper bound, it yields figures that are in good agreement with an established and conservative approach.

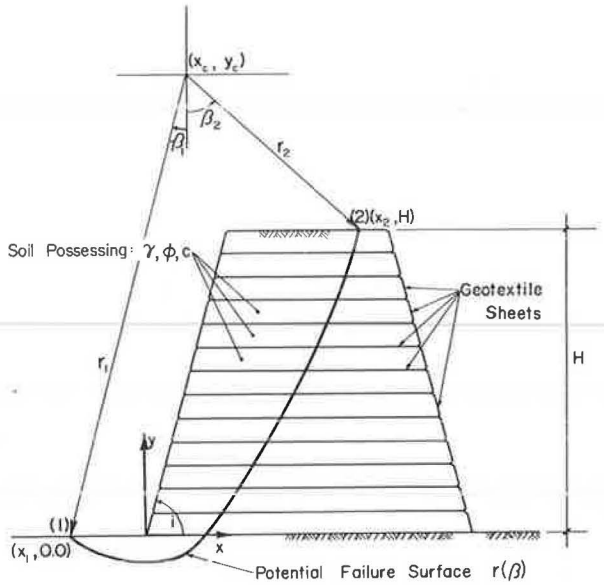

FIGURE 1 Notation and schematic presentation of the problem.

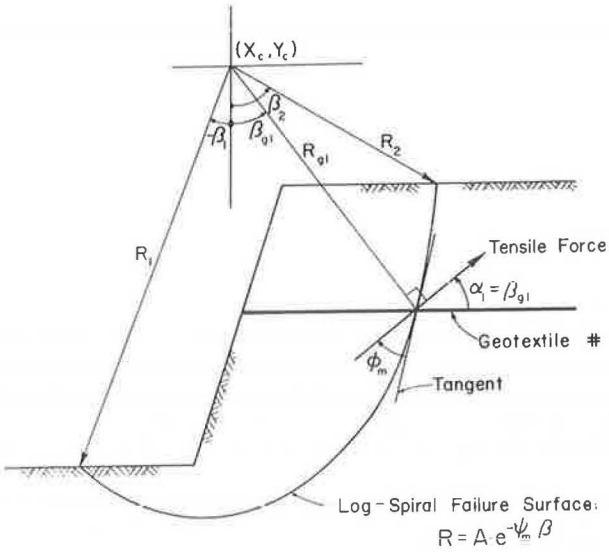

FIGURE 2 The failure mechanism described by Equations 4, 5, and 8.

ANALYSIS OUTLINE

Figure 1 shows a gravity wall on the verge of collapse. The wall is composed of soil wrapped in reinforcing geotextile sheets. The soil possesses unit weight γ, cohesion c, and friction angle ϕ. The height of the geotextile-reinforced wall is H and the general inclination of its face is i. A potential slip surface, expressed by an unknown function $r(\beta)$, initiates at the crest level [point (2)] and exits the soil mass at the toe level [point (1)]. Note that the slip surface is defined relative to a polar coordinate system that has its origin at some unknown point (x_C, y_C). As a consequence, points (1) and (2) are defined by the two unknown variables denoted as β_1 and β_2. The potential failure surface is acted on by two unknown distributed stresses: normal $[\sigma(\beta)]$, and shear $[\tau(\beta)]$. It is assumed that geotextile j has zero flexural rigidity and it can carry, in its planar direction, only a tensile force of known magnitude t_j. This force, however, is inclined at an unknown angle α_j and is acting at the geotextile's intersection with the slip surface (see Figure 2).

To attain the state of limiting equilibrium (i.e., verge of failure), the shear resistance developed over the slip surface must be fully mobilized. This condition, however, rarely occurs. Therefore, the common concept of limited mobilization of shear resistance is adopted. As a result, a stable system can now realize the limiting equilibrium state. By utilizing Coulomb's failure criterion and scaling down the components that strictly resist collapse (i.e., τ and t_j) so that limit equilibrium is artificially attained, the following equations result:

$$\tau_m = (c + \sigma\psi)/F_s \quad (1)$$

$$t_{m_j} = t_j/F_s \tag{2}$$

where

F_s = an unknown reduction factor termed "factor of safety";
τ_m and t_m = the mobilized soil shear strength and mobilized geotextile tensile strength, respectively; and
$\psi = \tan\phi$.

For a given problem, the minimum value of F_s is sought. When F_s is a minimum, it is then the conventional factor of safety commonly used in limit equilibrium analysis. In the physical sense, F_s quantifies the margin of safety with respect to available shear strength. Note, however, that F_s is applied equally to the soil (cohesion and friction) strength and the geotextile tensile strength, and that its value is constant for the entire slip surface. This is consistent with the averaging nature of the limit-equilibrium approach.

It should be pointed out that because a composite structure is being analyzed, which is made up of materials possibly exhibiting different stress-strain characteristics, the materials' strength parameters (Equations 1 and 2) should be determined on the basis of a limiting strain value that is identical for all materials. In most cases, however, this limiting value should correspond to the soil's shear deformation at failure rather than to the geotextile's tear strength, which may occur at relatively large elongation. Note that similar considerations are frequently used in determining the strength parameters of a layered soil profile for the purpose of limiting-equilibrium slope stability analysis. Further discussion of this important topic, however, is beyond the scope of the present work.

It can be verified (13) that by satisfying all equilibrium equations for a potentially sliding body (e.g., for which Equations 1 and 2 are valid) while extremizing F_s by using variational techniques, the following results are obtained:

$$R = A\exp^{(-\psi_m \beta)} \tag{3}$$

$$S = [A/(1 + 9\psi_m{}^2)]\ (\cos\beta + 3\psi_m \sin\beta)\exp^{(-\psi_m \beta)} - N_m\left\{[1 - \exp^{(2\psi_m \beta)}]/\psi_m\right\} + B\exp^{(2\psi_m \beta)} \quad \text{for } \psi_m \neq 0 \tag{4}$$

$$S = A\cos\beta + 2N_m\beta + B \quad \text{for } \psi_m = 0 \tag{5}$$

$$\alpha_j = \beta_{g_j} \tag{6}$$

where

A and B = unknown constants;
R = r/H is the nondimensional representation of the potential slip surface r, defined relative to a polar coordinate system having its origin at an unknown point (X_C, Y_C) where $X_C = x_C/H$ and $Y_C = y_C/H$ (see Figure 2);
$\psi_m = (\tan\phi)/F_S$;
$N_m = c/(F_S\gamma H)$;
S = $\sigma/\gamma H$ is the nondimensional representation of the normal stress distribution $\sigma(\beta)$ over $R(\beta)$; and
β_{g_j} = the angle defining the intersection of geotextile j and the slip surface R.

Equations 3-5 were previously obtained by Baker and Garber (11). Equation 3 represents a log-spiral slip surface and Equation 6 indicates that the geotextile is orthogonal to the radius vector defining it at its intersection with the slip surface. The failure mechanism described by these two equations is shown in Figure 2. Note that this mechanism is identical to rigid body rotational failure used in limit analysis where the velocity is opposing the geotextile tensile force (15).

The geotextile tensile strength is not explicitly expressed in Equations 3-5, indicating that the nature of R and S is not affected by t_j. The force t_j, however, appears in the equilibrium equations together with R and S. Satisfaction of equilibrium implies that the constants A and B, defining S and R, depend on t_j. As a consequence, the slip surface location and magnitude of the normal stress are linked to t_j.

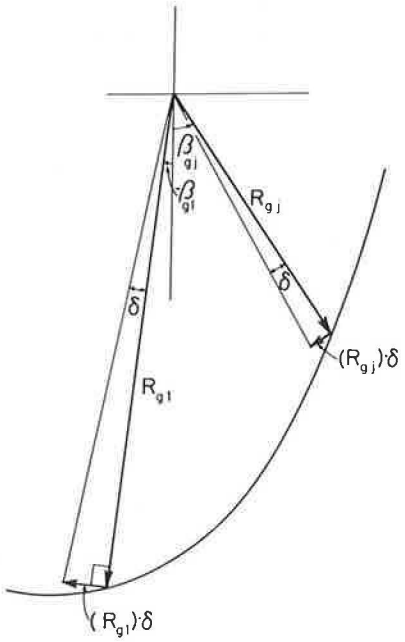

FIGURE 3 Virtual rotation of a rigid body.

In considering the virtual rotation of a rigid body combined with the derived failure mechanism, it can be shown that the geotextiles do not tend to stretch uniformly unless the log-spiral degenerates into a circle (see Figure 3). Because of the slip surface geometry, the geotextile at the lowest elevation, which is denoted as 1 in Figure 3, will elongate the most and therefore it is assumed that this geotextile will reach its tensile strength t_1 first. From a strict limiting equilibrium viewpoint, once t_1 is fully developed, a collapse resembling a row of dominoes falling down will occur; that is, all other geotextiles will fail one after the other in an upward orderly manner. It implies that as geotextile 1 is approaching its strength t_1, all other geotextiles are not necessarily on the verge of collapse and therefore their tensile force at that instance needs to be specified. In assuming that up to the elongation that corresponds to t_1, the load-elongation relationship is linear and by utilizing the mechanism shown in Figure 3, the adjusted tensile force relative to t_1 can be written as

$$t_j = t_1 \exp^{[-\psi_m (\beta_{g_j} - \beta_{g_1})]} \quad (7)$$

where t_1 is the geotextile's actual tensile strength, fully developed in the geotextile at the lowest elevation; and t_j is the tensile force developed in geotextile j at the same instant that t_1 is fully mobilized.

At this time, it is convenient to convert the force per unit length t_j into the following nondimensional expression:

$$T_{m_j} = (1/\gamma H^2)(t_j/F_s) = \left\{\exp^{[-\psi_m (\beta_{g_j} - \beta_{g_1})]}/\gamma H^2\right\}(t_1/F_s)$$
$$= T_{m_1} \exp^{[-\psi_m (\beta_{g_j} - \beta_{g_1})]} \quad (8)$$

where T_{m_j} is the nondimensional tensile force of geotextile j.

It can be verified (13) that for given i, ψ_m, T_{m_1}, and elevations of all geotextiles (i.e., β_{g_j}), the following unknown constants exist: X_c, Y_c, A, B, N_m β_1, β_2, and T_{m_j} (j = 2,3...n). The necessary equations can be obtained by essentially following a procedure developed by Baker (16). These equations consist of

1. Three equations of limiting equilibrium;
2. Two equations representing geometrical boundary conditions, i.e., $Y(X_1) = 0$ and $Y(X_2) = 1$;
3. Two equations resulting from extremization of $R(\beta)$ and $S(\beta)$ at the boundaries [transversality conditions (11)]; and
4. Equation 8 multiplied by (n - 1) where n is the number of geotextile sheets.

For a given i, ψ_m, T_{m_1}, and geotextiles' elevation (i.e., β_{g_j}), the required nondimensional cohesion N_m can be determined by solving these equations.

RESULTS

The analysis outlined before was used to gain some insight into the geotextiles' reinforcing effects and to generate design charts. It appears that the following definition of equivalent tensile strength is useful when a number of geotextiles are involved:

$$T_m = n \times T_{m_1} \quad (9)$$

where

n = the number of equally spaced geotextiles,
T_{m_1} = the nondimensional tensile strength of the geotextile placed at the toe elevation, and
T_m = the nondimensional equivalent tensile strength.

All the results presented here are based on analysis of walls reinforced by 10 horizontal and equally spaced geotextiles (n = 10). Some walls reinforced by 2 or 40 geotextiles were also analyzed. When the equivalent strength T_m was the same for n = 2, 10, or 40, the generated results exhibited insignificant differences. It can therefore be concluded that, in effect, the results presented here are general and applicable (when appropriate) for any number of horizontal and equally spaced geotextiles. This conclusion is limited to $n \geq 2$ where the first geotextile is placed at the toe elevation.

Figures 4-7 show typical distributions of tensile forces developed in a set of geotextiles. Note that the soil strength parameters are substituted by a single parameter $\lambda_{c\phi}$, defined for a system on the verge of collapse (i.e., for a given T_m) as

$$\lambda_{c\phi} = N_m/\psi_m = (1/\gamma H)(c/\tan\phi) \quad (10)$$

Figures 4-7 show that for a highly cohesive soil (e.g., $\lambda_{c\phi} = 100$), where the developed slip surface closely resembles a circular arc, all geotextiles are equally mobilized. In the case of a highly frictional soil (e.g., $\lambda_{c\phi} = 0.1$), however, there is a significant decrease in the geotextiles' tensile strength mobilization as their elevation approaches the crest. This decrease is more pronounced as the inclination of the wall's face decreases.

Figures 8 and 9 show the effect of the geotextile tensile strength on the potential slip surface. Note that (a) the larger the T_m, the deeper the slip surface regardless of the soil strength parameters; (b) the effect of T_m increases as i decreases (this is particularly true when cohesive soil is involved), and (c) the more cohesive the soil, the deeper the slip surface.

Figures 10 and 11 show some typical nondimensional normal stress distributions. It is interesting to note that as the critical slip surface is shifted by the geotextile reinforcement, there is

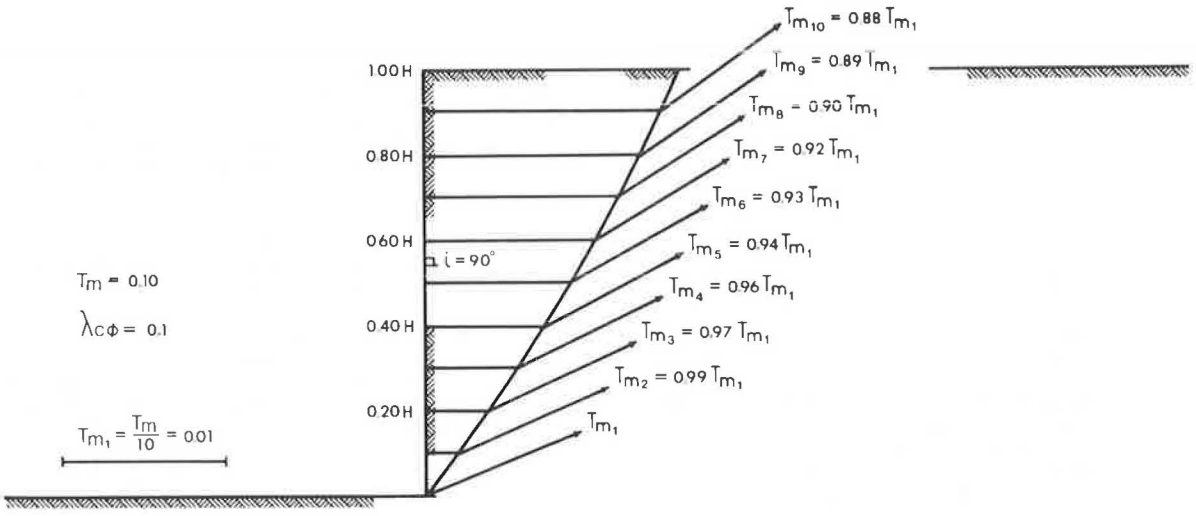

FIGURE 4 Typical distribution of geotextile tensile force for the case i = 90 degrees and T_m = .10 for highly frictional soil.

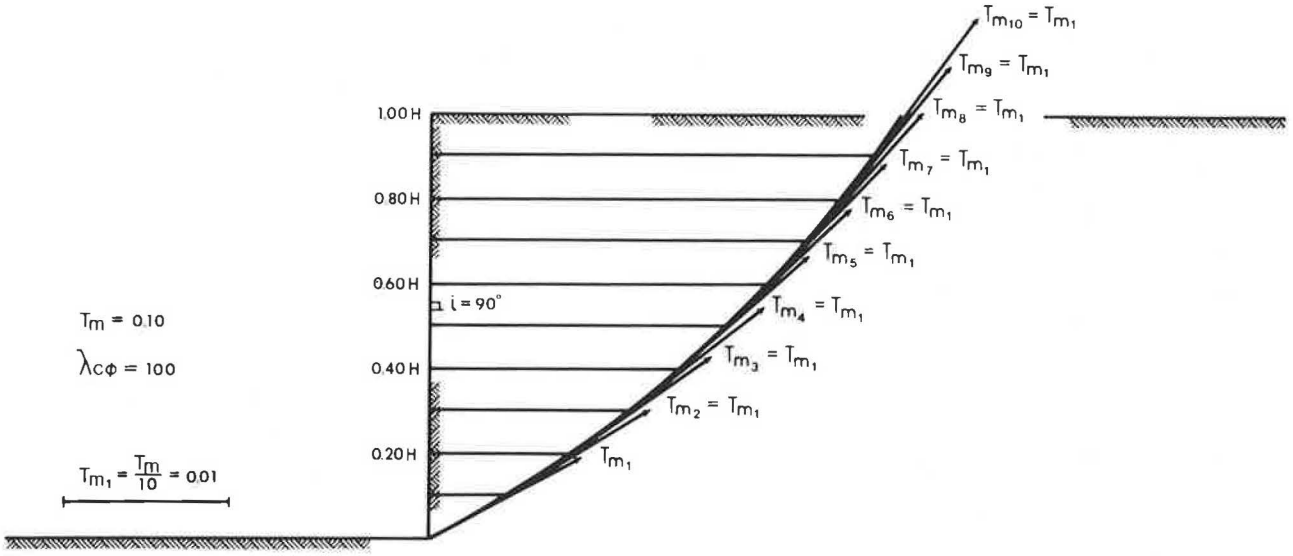

FIGURE 5 Typical distribution of geotextile tensile force for the case i = 90 degrees and T_m = .10 for highly cohesive soil.

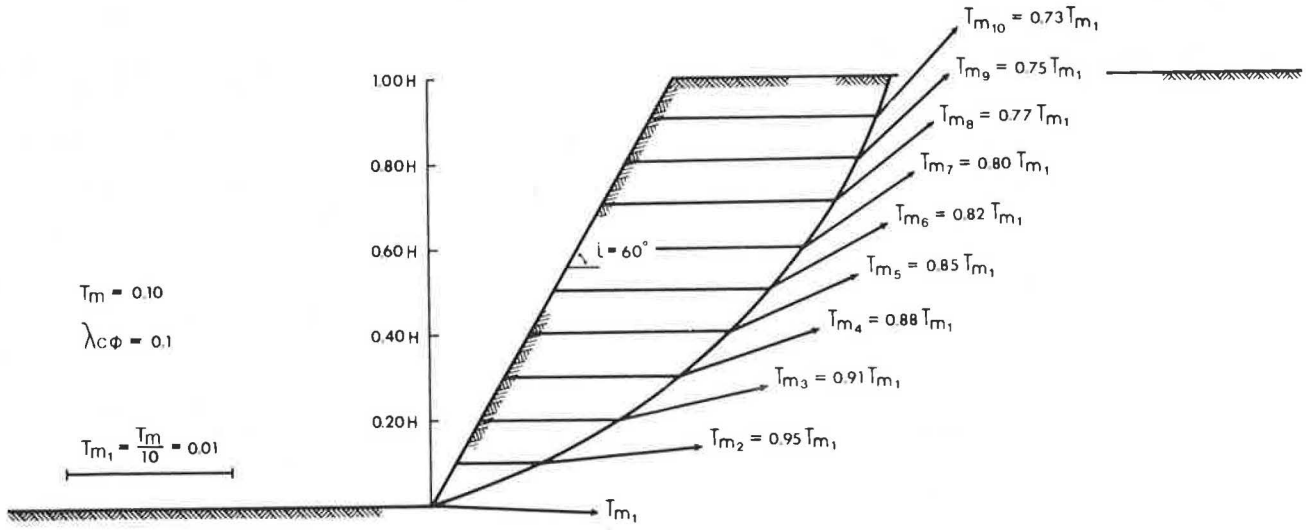

FIGURE 6 Typical distribution of geotextile tensile force for the the case i = 60 degrees for highly frictional soil.

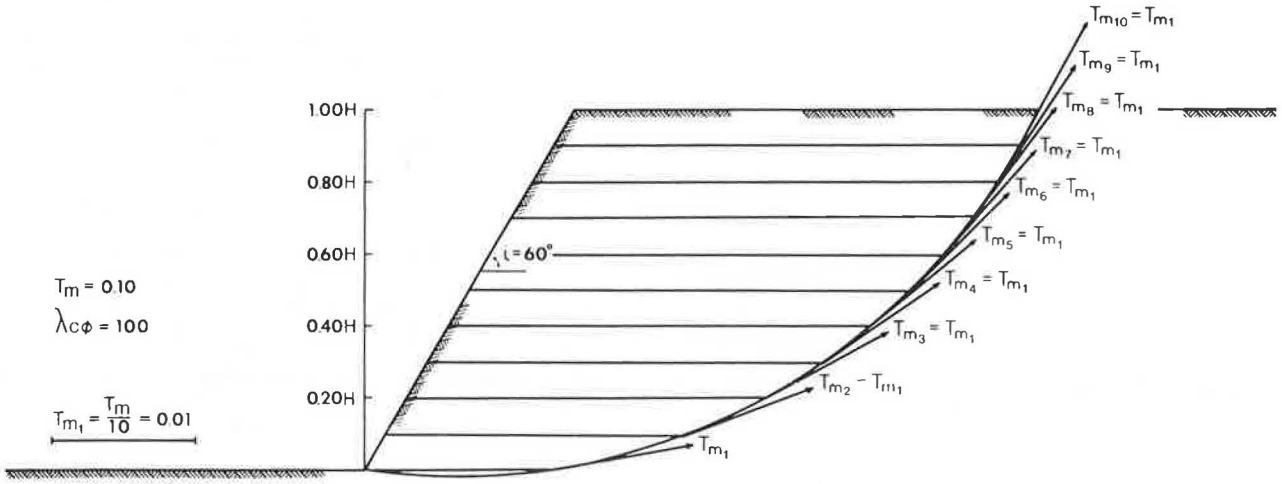

FIGURE 7 Typical distribution of geotextile tensile force for the case i = 60 degrees for highly cohesive soil.

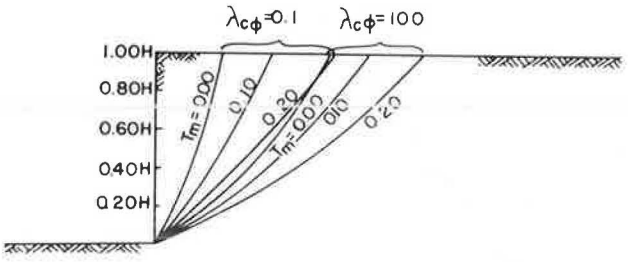

FIGURE 8 Typical effect of geotextile tensile strength on slip surface with a wall inclination of i = 90 degrees.

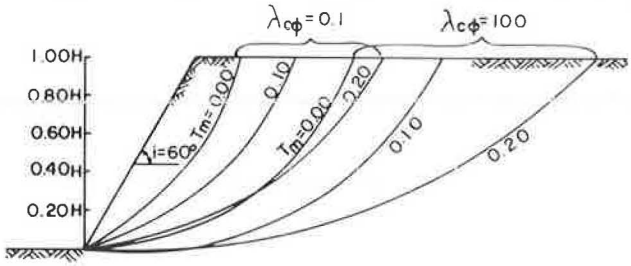

FIGURE 9 Typical effect of geotextile tensile strength on slip surface with a wall inclination of i = 60 degrees.

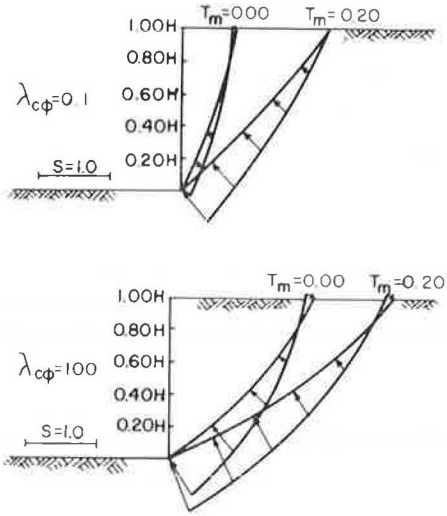

FIGURE 10 Typical effect of geotextile reinforcement on normal stress distribution with a wall inclination of i = 90 degrees.

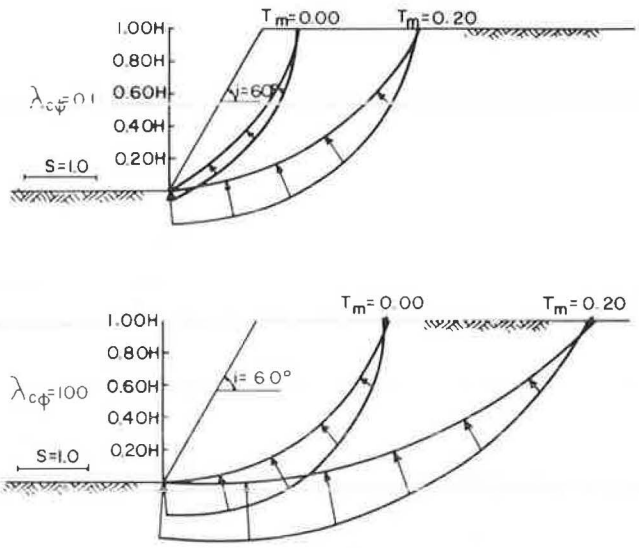

FIGURE 11 Typical effect of geotextile reinforcement on normal stress distribution with a wall inclination of i = 60 degrees.

(a) an increase in the magnitude of the compressive stress NORMAL to the critical slip surface, (b) a decrease in the magnitude of the soil's tensile stress at the crest (a region where tension cracks tend to develop), and (c) a decrease in the arc length along which this tensile stress is acting. The end result of these factors is an increase in the wall stability. It may be pointed out that tensile stress in soil is theoretically possible based on the validity of the Coulomb failure criterion and its magnitude is limited to $\sigma \geq - c/\tan\phi$. Although the existence of this failure criterion in the negative range of σ (or S) is questionable, it was assumed in the analysis that the criterion is valid for the entire range of $\sigma \geq - c/\tan\phi$. A modification of the analysis, however, can easily be carried out by following the procedure used by Baker (16).

Figures 12-14 show design charts for walls inclined at 60, 75, and 90 degrees. These charts can be used to determine the factor of safety of a given reinforced wall or, alternatively, be used to design a wall. Further elaboration about the application of the design charts is given in the next section.

Note that all the charts possess the same unique point on the ordinate ($\phi_m = 0$). At this point N_m equals 0.1810 and the critical slip surface is infinitely deep. The design charts indicate that for deep failure (slip surface passing below the toe), as ϕ_m decreases, the corresponding value of N_m converges to 0.1810 for any T_m greater than a certain value. This implies that under some conditions, the geotextile strength has very little or no effect on the stability. It should be stated that this phenomenon occurs together with an increase in the slip surface depth. It may therefore be concluded that as the mass of the sliding body increases, the significance of the geotextile reinforcement in preventing failure decreases. At the extreme case in which infinite failing mass is considered, a finite value of T_m is negligible and the required N_m equals 0.1810. Note that infinite failures (correspond to $N_m = 0.1810$) are typical to flat, cohesive, and unreinforced slopes (17). It should be pointed out, however, that assigning any small value to ϕ_m will result in a finite extension of the slip surface. In the event that deep failure is unlikely to develop, one still can use the design charts. The curves representing failure surfaces passing through the toe (dashed lines) are extended backwards based on computations for a noncritical case where failure is forced to pass through the toe.

The design charts were developed for the case where the failure surface initiates at the crest elevation and exits at the toe elevation, passing through all geotextile sheets. This, however, may not always be the critical case, especially when retaining walls are concerned, and therefore a numerical procedure is then necessary (13). To use the design charts presented here, a check must be made to determine whether the resulting critical slip surface can be realized for a given problem as was assumed in the analysis (e.g., to determine whether x_2 extends beyond the wall's crest, for which the

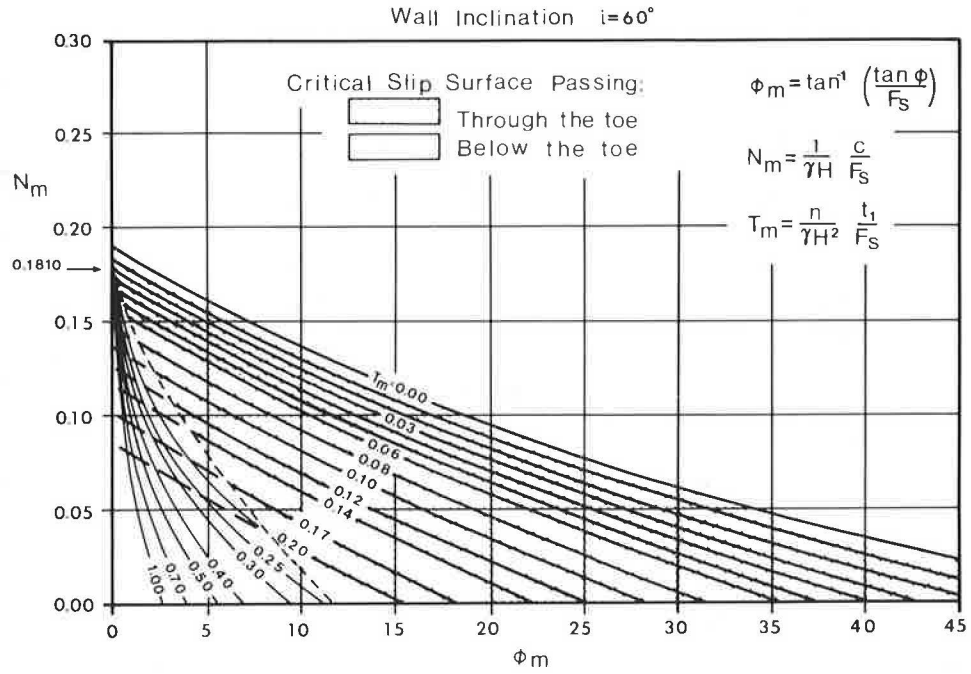

FIGURE 12 Design chart for 60-degree wall.

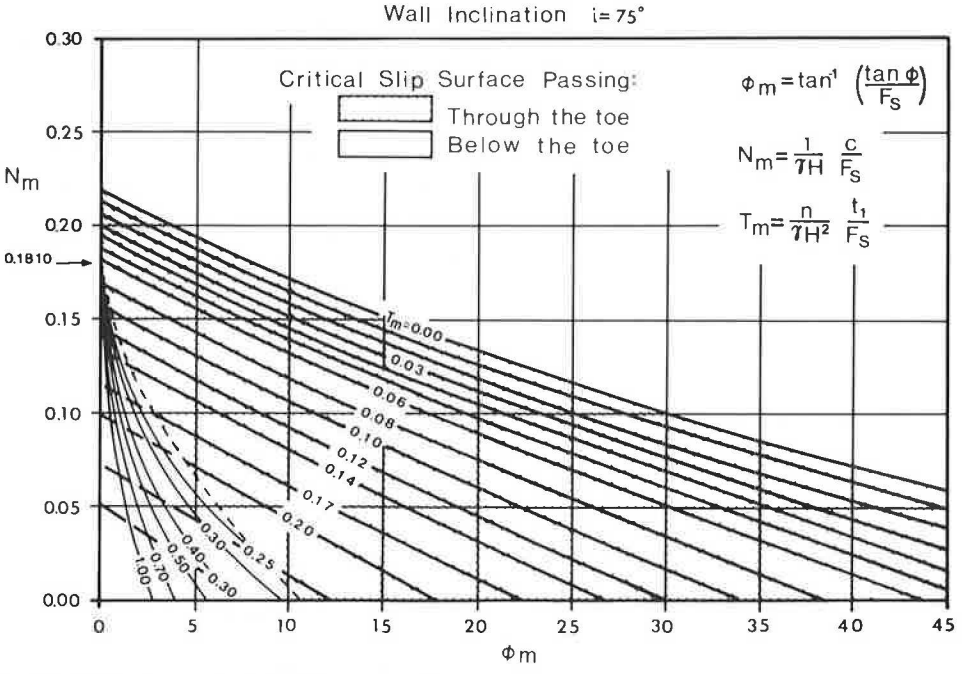

FIGURE 13 Design chart for 75-degree wall.

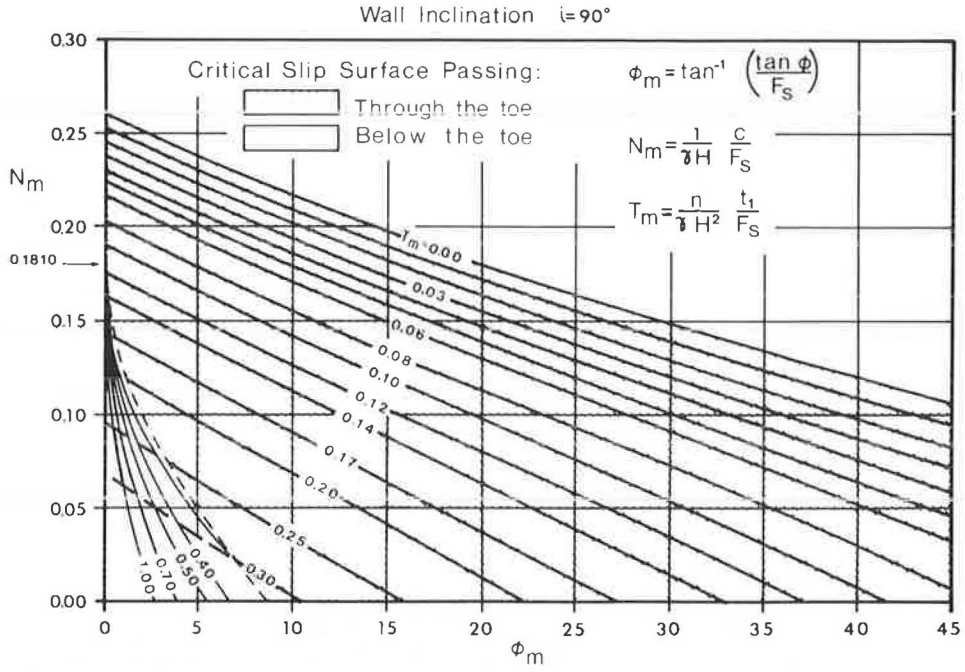

FIGURE 14 Design chart for 90-degree wall.

results are not then valid). Figure 15 shows some basic parameters that are used to define a slip surface exiting at the toe (i.e., $x_1 = y_1 = 0.0$). For this case, the parameters used are x_2, $y_2 = H$, and θ_2 where θ_2 is the angle of the tangent to the slip surface at (X_2, Y_2). From the geometry of the problem, the following can be obtained:

$$\beta_2 = \theta_2 - \phi_m \tag{11}$$

It can be verified that the following parametric equations, relating the polar and Cartesian coordinate system, exist:

$$X = X_c + A\exp^{(-\psi_m \beta)}\sin\beta \tag{12}$$

$$Y = Y_c - A\exp^{(-\psi_m \beta)}\cos\beta \tag{13}$$

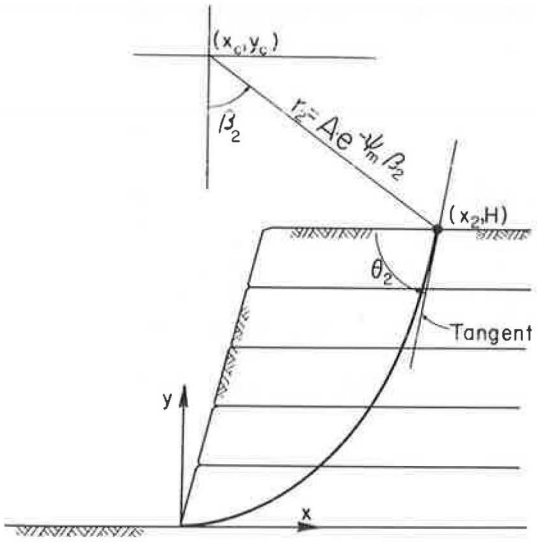

FIGURE 15 The parameters used in Figures 16-18 to define the slip surface.

Figures 16 through 18 provide all the information needed to determine the slip surface trace for walls inclined at i = 60, 75, and 90 degrees. Once ϕ_m, N_m, and T_m are determined for a given problem, θ_2 and x_2 (for which $x_1 = y_1 = 0.0$ and $y_2 = H$) can be evaluated from the corresponding figure (i.e., Figures 16-18). By combining Equations 11-13 with the preceding data, five equations will result that contain the following unknowns: A, X_c, Y_c, β_1, and β_2. By solving these five equations, the slip surface can be fully defined. As a consequence, a check can then be made to determine whether the predicted slip surface can be physically developed for the given problem.

ILLUSTRATIVE EXAMPLE

Consider the following design problem: A vertical geotextile-reinforced gravity wall is to be constructed to H = 20 ft high. The soil properties are γ = 120 lb/ft^3, ϕ = 35 degrees, and c = 275 lb/ft^2. The required tensile strength of the geotextiles, so that F_s = 1.5, is sought. For F_s = 1.5, the mobilized soil strength parameters are $\phi_m = \tan^{-1}(\tan\phi/F_s)$ = 25 degrees and $N_m = c/(F_s\gamma H)$ =0.076. By using Figure 10, it follows that the required T_m equals 0.10. The selection of 20 equally spaced geotextile sheets n = 20 (1 per foot) will result in a specified strength of $t_1 = (\gamma H^2)(F_s T_m)/n$ = 360 lb/ft. By using Figure 18 ($\lambda_{c\phi}$ = 0.076/tan 25 degrees = 0.163) and solving Equations 11-13, the following slip surface is predicted: $x_1 = y_1 = 0.0$, x_2 = 0.66 H = 13.2 ft, y_2 = H = 20 ft θ_2 = 65 degrees, β_2 = 40 degrees, x_c = 30.8 ft, y_c = 72.0 ft, A = 94.6 ft, and β_1 = 23 degrees.

Let us assume now that the wall was eventually constructed by using n = 30 equally spaced geotextile sheets each possessing a tensile strength of 300 lb/ft (t_1 = 300 lb/ft). The factor of safety needs to be determined for this case. If it is assumed that F_s = 2, then ϕ_m equals 19.3 degrees and can be expressed as

$$T_m = nt_1/(F_s\gamma H^2) = 0.094$$

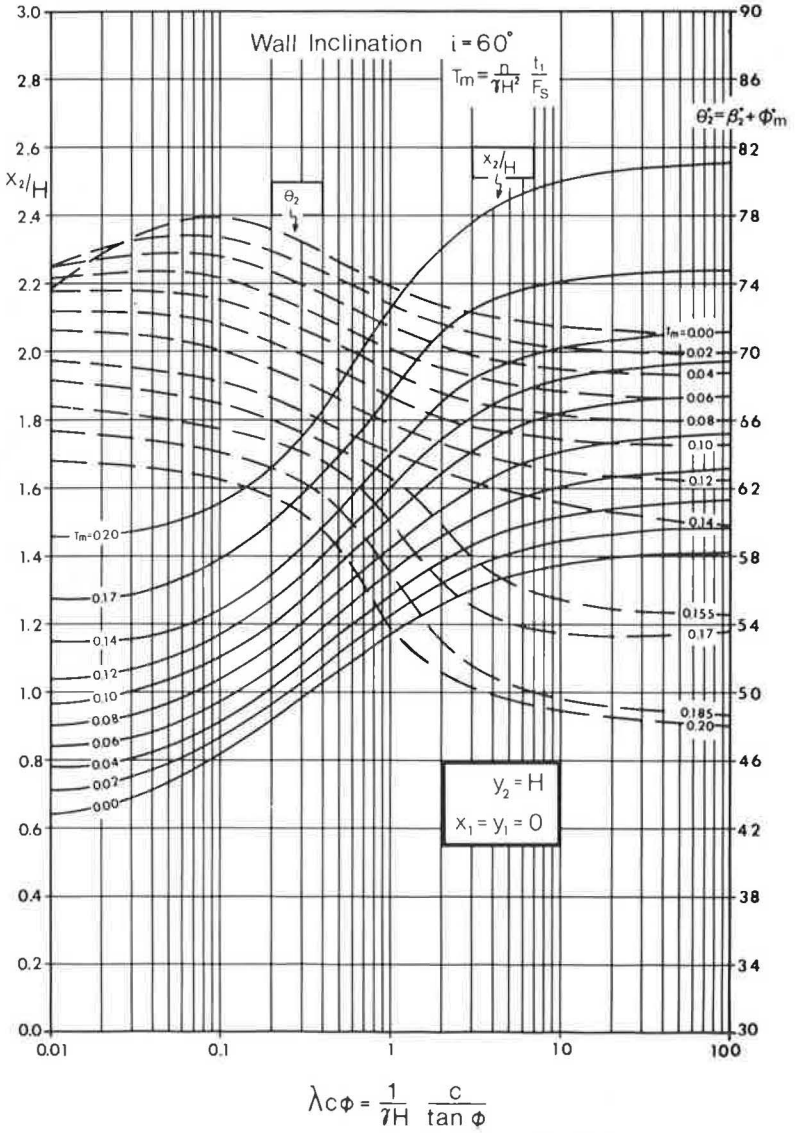

FIGURE 16 Parameters defining the slip surface where i = 60 degrees.

By using Figure 14, it follows that the required N_m is 0.106; the computed N_m, based on the given cohesion and the assumed F_S, is represented as

$$N_m = c/(F_S \gamma H) = 0.057$$

A new F_S must be assumed and the procedure is repeated until the assumed F_S produces a required N_m (see Figure 10) equal to the actual N_m, indicating that all strength components are indeed equally mobilized. It can be verified that for the given problem, F_S = 1.63.

It is interesting to note that an unreinforced slope, inclined at i = 53 degrees, and possessing identical soil (i.e., ϕ = 35 degrees, c = 275 lb/ft^2, and γ = 120 lb/ft^3), will have the same factor of safety (i.e., F_S = 1.63) as this vertical reinforced wall. This has clear engineering and economical implications in design and construction of stabilized embankments. It should be pointed out, however, that if the designed wall is used to retain backfill soil, its stability against overturning and base slide has to be checked by utilizing the common procedures for conventional retaining walls.

COMPARISON OF RESULTS

The results presented here are based on an approach that is equivalent to the upper bound theorem of plasticity. For a safe design, however, the lower bound generally is sought. Hence, to determine whether the method is useful for design purposes, some of the results must be compared with predictions produced by an extension of a limiting-equilibrium approach that is considered to be conservative when applied to unreinforced slopes.

Christie and El-Hadi (7) and Christie (18) modified the ordinary method of slices (Fellenius method) so that it would account for reinforcing-geotextile sheets. Although the geotextile tensile strength is mobilized by uneven deformations of the soil, Christie and El-Hadi conservatively assumed that the geotextile tensile force remains horizontal at the slip surface and considered the tensile force action as a uniform distributed force (per unit

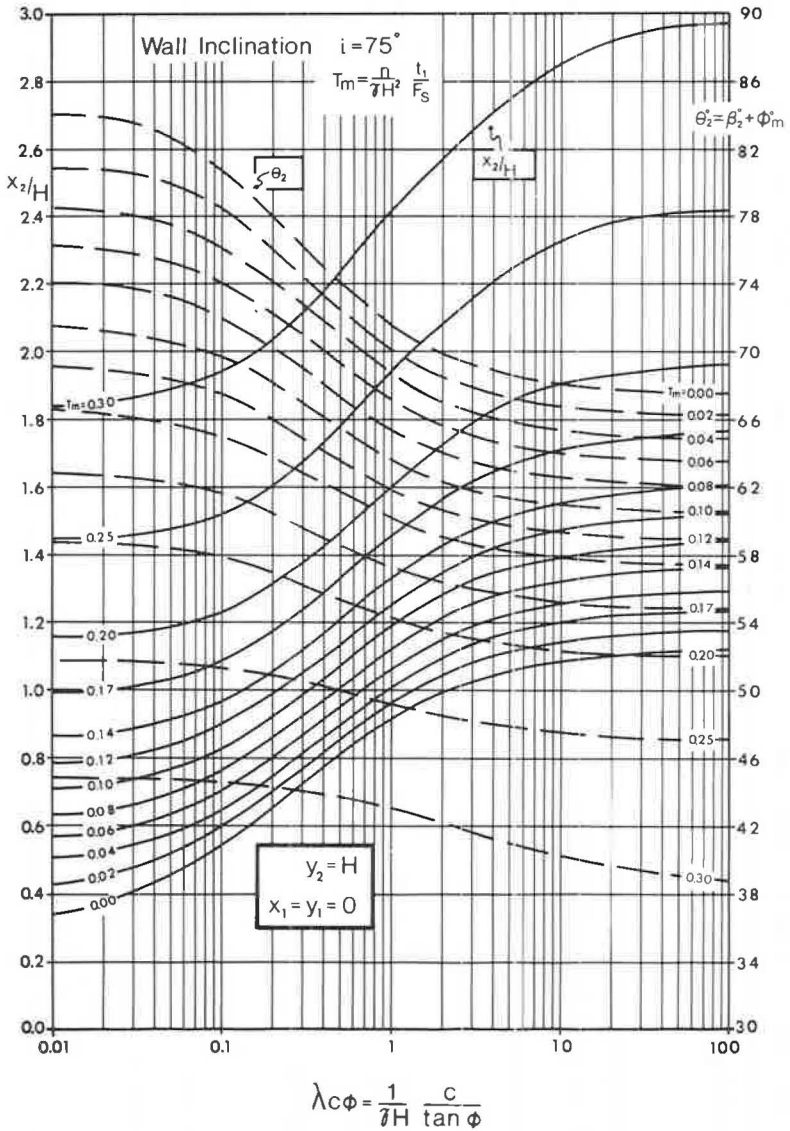

FIGURE 17 Parameters defining the slip surface where i = 75 degrees.

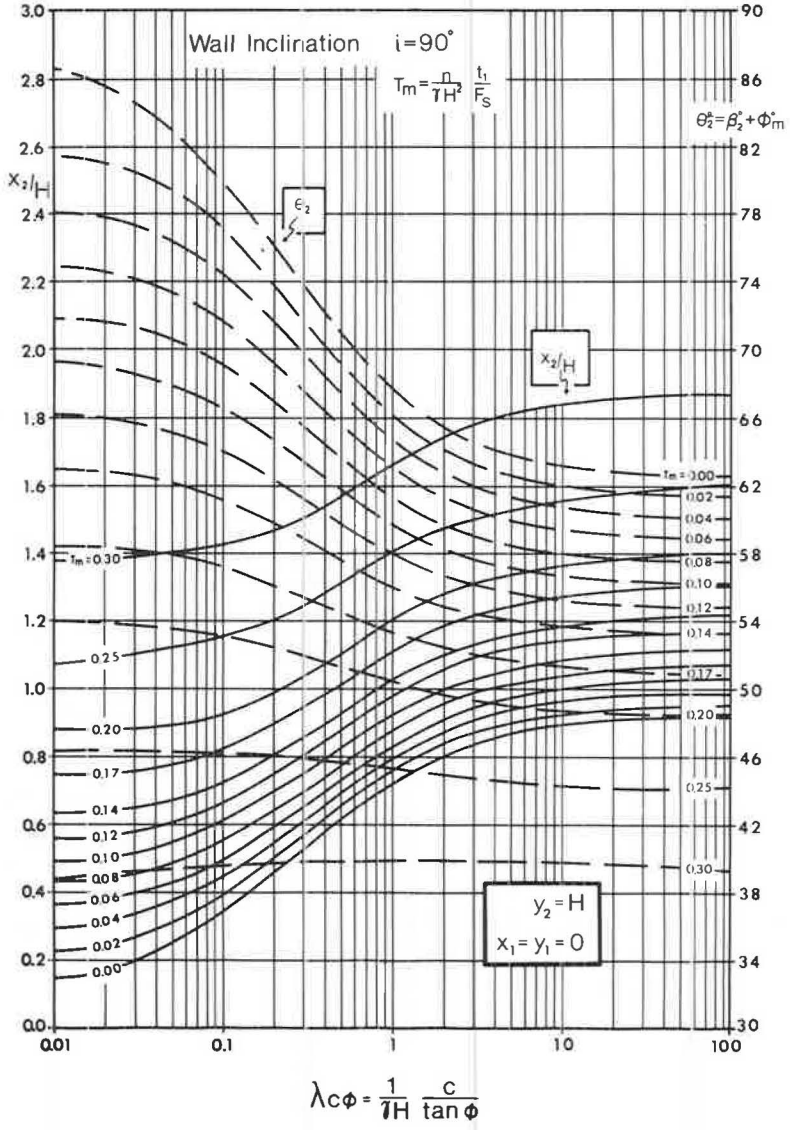

FIGURE 18 Parameters defining the slip surface where i = 90 degrees.

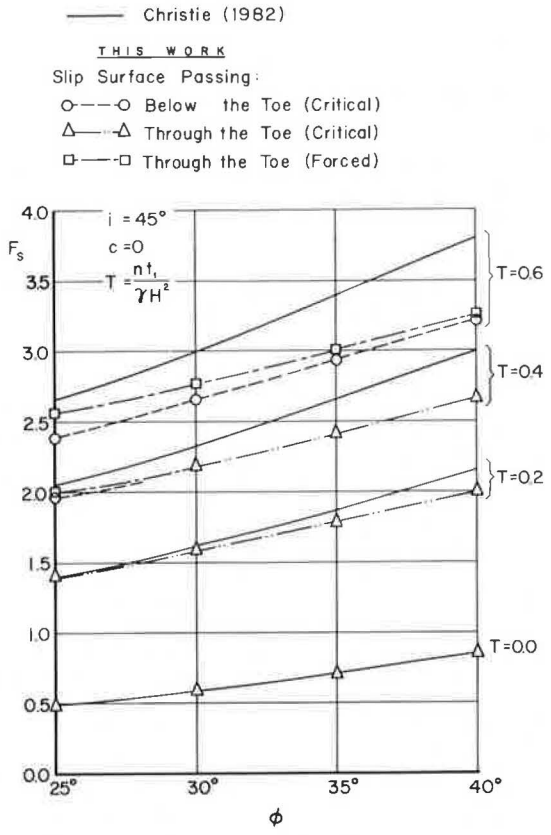

FIGURE 19 Comparison of results where c = 0.

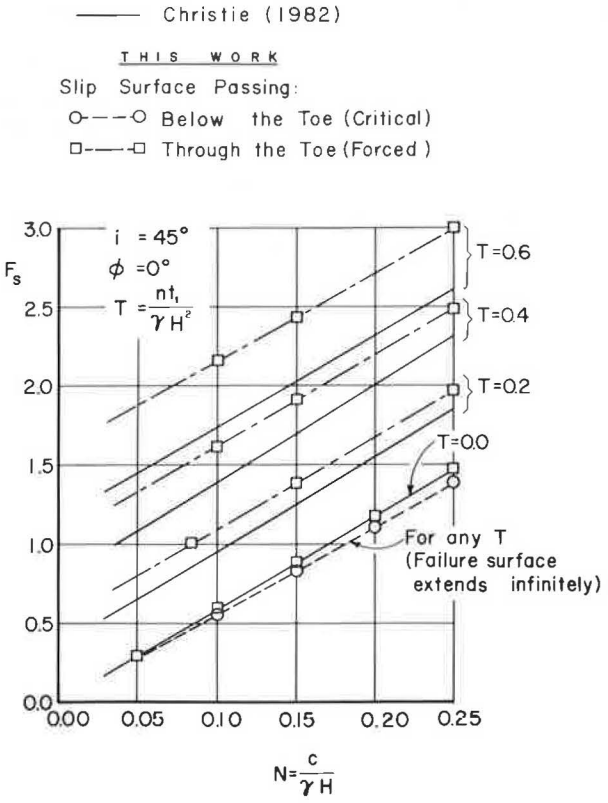

FIGURE 20 Comparison of results where $\phi = 0$.

height) rather than as a line load (7). Christie applied the safety factor equally to the geotextile tensile strength and soil strength (18), an approach that is also used in this work.

By using this modified Fellenius method, Christie analyzed a 66-ft high embankment with 45 degree side-slopes, subjected to undrained ($\phi = 0$) and drained ($c = 0$) conditions (18). A summary of Christie's and this work's normalized results is shown in Figures 19 and 20. Because it is not clear whether Christie's safety factors correspond to toe failure or represent the absolute minimum, the authors have presented their results for both cases (when appropriate)--minimum F_S when the failure surface (a) is forced to exit at the toe and (b) is mathematically the critical one.

Figure 19 shows that for the particular problem analyzed (i = 45 degrees, c = 0), the safety factors generated by this work are smaller (i.e., more critical), than Christie's, especially as the geotextile tensile strength or the friction angle increases. Figure 20, for which $\phi = 0$, implies that if no constraints are imposed on the slip surface, it will extend to infinity and, as discussed earlier, the geotextiles' finite strength is not relevant. This mode of failure is therefore the critical one because its corresponding safety factors are smaller. In the case of toe failure mode, however, Christie's results are smaller, provided his safety factors correspond to toe failure.

In considering realistic values of T, the differences in safety factors obtained for the given problem by using the two approaches are rather small. Although this work is employing a technique theoretically classified as upper bound, its results compare favorably with predictions produced by a conservative limiting-equilibrium approach (19), which was conservatively extended to include the geotextile reinforcement effect. It should be pointed out that predictions by an extension of the presented variational analysis are in good agreement with experimental results obtained by Leshchinsky (13).

CONCLUSIONS

Results of a mathematical approach to stability of geotextile-retained soil walls are presented. The analytical approach is based on limiting equilibrium combined with variational extremization. Because of the generality of the analysis, the results can also be applied to a wide range of problems of similar nature (e.g., the stability of geotextile-reinforced earth slopes). The analysis results indicate that the critical slip surface is log-spiral and that on the verge of failure, each geotextile sheet is orthogonal to the radius vector defining its intersection with the critical failure surface. To account for several geotextiles in a consistent manner, a methodology that employs a rigid body rotation was introduced.

Conclusions made on the basis of figures obtained through a closed-form solution, are as follows:

1. When a granular soil is concerned, there is a significant decrease in the mobilized strength of the geotextiles as their elevation approaches the crest.
2. As the geotextile strength increases, the extent of the critical slip surface increases. This effect is more pronounced as the wall face inclination decreases.
3. As the geotextile tensile strength increases (a) the compressive stress normal to the critical slip surface increases, and (b) the magnitude and

extent of tensile stress, typically acting near the crest, decreases.

The end products of this work are design charts that can easily be applied to a particular problem.

To verify whether the presented approach is acceptable at all, its results were compared with predictions based on a conservative extension of the ordinary method of slices as applied to a problem possessing similar characteristics to reinforced walls. The results compared favorably. The application of the variational approach, however, is easier. It should be noted that a closed-form solution can also be assembled for various types of loading conditions such as pore water pressures and surcharge loads. As a consequence, similar stability charts may be developed for these conditions. Furthermore, the analysis can be modified so that the geotextile spacing and strength can be specified individually in accordance with the investigated problem.

REFERENCES

1. J.R. Bell and J.E. Steward. Construction and Observations of Fabric Retained Soil Walls. Proc., International Conference on the Use of Fabrics in Geotechnics, Vol. 1, Paris, France, 1977, pp. 123-128.
2. G.E. Douglas. Design and Construction of Fabric-Reinforced Retaining Walls by New York State. In Transportation Research Record 872, TRB, National Research Council, Washington, D.C., 1982, pp. 32-37.
3. R.K. Rowe. Reinforced Embankments: Analysis and Design. Journal of the Geotechnical Engineering Division, ASCE, Vol. 110, No. 2, Feb. 1984, pp. 231-246.
4. D. Leshchinsky. AAR Geotextile Testing to Date. Railway Track and Structures, Vol. 78, No. 6, June 1982.
5. R.L. Nicholls. Comparison of Fabric Sheet-Reinforced Earth Design Methods. Canadian Geotechnical Journal, Vol. 18, 1981, pp. 585-592.
6. R.T. Murray. Fabric Reinforced Earth Walls: Development of Design Equations. Ground Engineering, Vol. 13, No. 7, 1980, pp. 29-36.
7. I.F. Christie and K.M. El-Hadi. Some Aspects of the Design of Earth Dams Reinforced with Fabric. Proc., International Conference on the Use of Fabrics in Geotechnics, Vol. 1, Paris, France, 1977, pp. 99-103.
8. R.T. Murray. Fabric Reinforcement of Embankments and Cuttings. Proc., 2nd International Conference on Geotextiles, Vol. 3, Las Vegas, Nev., 1982, pp. 707-713.
9. T.S. Ingold. An Analytical Study of Geotextile Reinforced Embankments. Proc., 2nd International Conference on Geotextiles, Vol. 3, Las Vegas, Nev., 1982, pp. 683-688.
10. R.A. Jewell. A Limit-Equilibrium Design Method for Reinforced Embankments on Soft Foundations. Proc., 2nd International Conference on Geotextiles, Vol. 3, Las Vegas, Nev., 1982, pp. 671-676.
11. R. Baker and M. Garber. Variational Approach to Slope Stability. Proc., 9th International Conference on Soil Mechanics and Foundation Engineering, Vol. 2, Tokyo, 1977, pp. 9-12.
12. R. Baker and M. Garber. Theoretical Analysis of the Stability of Slopes. Geotechnique 28. No. 4, 1978, pp. 395-411.
13. D. Leshchinsky. Geotextile Reinforced Earth. Parts I and II, Department of Civil Engineering, University of Delaware, Newark, Del., July 1984, Research Reports CE 84-44/45.
14. D. Leshchinsky, R. Baker, and M.L. Silver. Three Dimensional Analysis of Slope Stability. International Journal for Numerical and Analytical Methods in Geomechanics, Vol. 9, No. 3, 1985, pp. 199-223.
15. W.F. Chen. Limit Analysis and Soil Plasticity. Elsevier, Amsterdam, Netherlands, 1975.
16. R. Baker. Tensile Strength, Tension Cracks and Stability of Slopes. Soils and Foundations--Journal of the Japanese Society of Soil Mechanics and Foundations Engineering, Vol. 21, No. 2, 1981, pp. 1-17.
17. D.W. Taylor. Fundamentals of Soil Mechanics. John Wiley and Sons, Inc., New York, 1948.
18. I.F. Christie. Economic and Technical Aspects of Embankments Reinforced with Fabric. Proc., 2nd International Conference on Geotextiles, Vol. 3, Las Vegas, Nev., 1982, pp. 659-664.
19. A.W. Bishop. The Use of the Slip Circle in the Stability Analysis of Slopes. Geotechnique, Vol. 5, No. 1, 1955, pp. 7-17.

Publication of this paper sponsored by Committee on Task Force on Engineering Fabrics.